Published in final edited form as:
J Am Chem Soc. 2010 August 4; 132(30): 10414–10423. doi:10.1021/ja102775u.

Magic Angle Spinning NMR Analysis of β_2-Microglobulin Amyloid Fibrils in Two Distinct Morphologies

Galia T. Debelouchina[1,2], **Geoffrey W. Platt**[3,4], **Marvin J. Bayro**[1,2], **Sheena E. Radford**[3,4], and **Robert G. Griffin**[1,2]

Robert G. Griffin: rgg@mit.edu

[1] Department of Chemistry, Massachusetts Institute of Technology, Cambridge, MA 02139, USA

[2] Francis Bitter Magnet Laboratory, Massachusetts Institute of Technology, Cambridge, MA 02139, USA

[3] Astbury Centre for Structural Molecular Biology, University of Leeds, Leeds LS2 9JT, UK

[4] Institute of Molecular and Cellular Biology, University of Leeds, Leeds LS2 9JT, UK

Abstract

β_2-Microglobulin (β_2m) is the major structural component of amyloid fibrils deposited in a condition known as dialysis-related amyloidosis. Despite numerous studies that have elucidated important aspects of the fibril formation process *in vitro*, and a magic angle spinning (MAS) NMR study of the fibrils formed by a small peptide fragment, structural details of β_2m fibrils formed by the full-length 99-residue protein are largely unknown. Here, we present a site-specific MAS NMR analysis of fibrils formed by the full-length β_2m protein, and compare spectra of fibrils prepared under two different conditions. Specifically, long straight (LS) fibrils are formed at pH 2.5, while a very different morphology denoted as worm-like (WL) fibrils is observed in preparations at pH 3.6. High-resolution MAS NMR spectra have allowed us to obtain ^{13}C and ^{15}N resonance assignments for 64 residues of β_2m in LS fibrils, including part of the highly mobile N-terminus. Approximately 25 residues did not yield observable signals. Chemical shift analysis of the sequentially assigned residues indicates that these fibrils contain an extensive β-sheet core organized in a non-native manner, with a *trans*-P32 conformation. In contrast, WL fibrils exhibit more extensive dynamics and appear to have a smaller β-sheet core than LS fibrils, although both cores seem to share some common elements. Our results suggest that the distinct macroscopic morphological features observed for the two types of fibrils result from variations in structure and dynamics at the molecular level.

Introduction

More than twenty-five different proteins are known to form amyloid fibrils that are observed to accumulate in a range of human and animal diseases.[1] Additionally, proteins and peptides that are not involved in disease states can be induced to form amyloid-like fibrils *in vitro*, indicating that formation of these ordered aggregates is potentially a generic attribute of all protein sequences.[2] These fibrils share common morphological features in that they are long, straight and unbranched, and are formed from multiple protofilaments arranged with a twisted organisation.[3] Higher resolution analyses reveal that the fibrils consist of a cross-β architecture, which involves the formation of β-strands oriented perpendicular to the fibril

Supporting Information Available
EM images of LS fibrils and WL fibrils before and after buffer change, medium range ^{15}N-^{13}C correlation experiments of LS fibrils. This material is available free of charge *via* the Internet at http://pubs.acs.org.

long axis and imparts the characteristic tinctorial properties of all amyloid fibrils, specifically that they bind small fluorescent molecules such as thioflavin-T and Congo Red.[4–6] X-ray crystallography has provided insight into the cross-β structural arrangement of crystals formed by short amyloidogenic peptides where the sidechains pack in a tight, self-complementing manner referred to as a "steric zipper".[7] Magic angle spinning (MAS) NMR studies on these and other systems have shown, however, that amyloid structures can be much more complex[8] and that other structural arrangements such as the β-solenoid are also possible.[9] Indeed, structural models primarily based on MAS NMR data have emerged for a number of different systems including Aβ(1–40),[10] a 22-residue segment of β_2-microglobulin,[11] amylin,[12] α-synuclein,[13,14] HET-s(218–289),[9] etc., and have provided valuable information regarding the common principles and interactions that govern fibril architecture. Our understanding of the structural molecular process of amyloid formation is, however, far from complete and improved knowledge in this area will not only enable design of therapeutic strategies against protein aggregation diseases,[15] but it will also allow for the useful biotechnological properties of protein aggregation to be harnessed.[16]

The protein β_2-microglobulin (β_2m), is the major structural component of amyloid fibrils associated with dialysis-related amyloidosis.[17] The protein is 99 residues in length (with an additional N-terminal Met0 in the recombinant protein), that folds natively into a β-sandwich conformation, where a disulphide bond between C25 and C80 covalently links the sheets.[18] A number of studies have described the formation of amyloid-like fibrils from full-length β_2m *in vitro* under a range of conditions, including the addition of co-solvents and metal ions.[19] Canonical long-straight (LS) amyloid-like fibrils (~1 μm long) have been observed to form *in vitro* from oxidized β_2m under aqueous conditions at both pH 7,[19,20] where the native globular state is initially populated, and under acidic conditions (pH < 3), where the β_2m polypeptide initially adopts a highly dynamic acid-unfolded state.[21–23] The presence of an intact disulphide bond is a necessity for formation of these fibrils that, in common with amyloid formed from many different proteins, grow with lag-dependent kinetics, consistent with a nucleated assembly mechanism. However, if the same oxidized β_2m is incubated under low pH conditions in the presence of increased ionic strength (≥ 100 mM) shorter (~150–600 nm) curvilinear fibrils, which have previously been described as worm-like (WL), form *via* a kinetic pathway that lacks a lag phase.[19] Previous studies indicate that the LS and WL fibrils are morphologically distinct, for example they have different persistence lengths, different responses to ThT and Congo Red and give rise to fibril diffraction patterns consistent with highly ordered and less well ordered fibrillar samples, respectively.[19,24] Furthermore, LS fibrils have been shown by hydrogen exchange (HX) and limited proteolysis studies to have a more extensively and highly protected core than that of WL fibrils.[25,26] Recent analyses of the β_2m fibrils have provided some structural information, for instance, cryoEM studies of the LS β_2m fibrils have indicated formation of a complex structure based on the stacking of globular units organized as six protofilaments arranged in two crescent-like filaments.[27] Data from FTIR and EPR measurements of the LS fibrils have suggested that the cross-β structure of the polypeptide chain within these fibrils shows a parallel and in-register arrangement.[28–30] Interestingly, EPR data indicate that β_2m WL fibrils do not adopt such a highly organized structure.[30]

Here, we describe the initial MAS NMR analysis of LS and WL amyloid-like fibrils prepared *in vitro* from the full-length sequence of β_2m and discuss preliminary chemical shift assignments of the β_2m sequence in LS fibrils formed at low pH. Our data shed light on the regions of the protein sequence involved in the rigid core of the fibrils and the secondary structure present in these segments when arranged in the fibrillar state. In addition, we compare the spectra of LS fibrils with those obtained from WL fibrils, to determine whether the gross morphological differences can be explained by atomic level structural differences.

Results

Resonance assignment of LS β_2m fibrils

In order to assign sequentially the resonances in the long straight (LS) β_2m fibrils formed at pH 2.5 and low ionic strength (see Methods and Figure S1) we relied on a set of ^{13}C-^{13}C and ^{15}N-^{13}C correlation spectra recorded with three differently labeled samples: uniformly ^{13}C, ^{15}N labeled β_2m fibrils (U-β_2m), and two samples prepared by growing bacteria in media containing [2-^{13}C]-glycerol (2-β_2m) or [1,3-^{13}C]-glycerol (1,3-β_2m) as the ^{13}C source.[31–33] Figure 1 shows a typical ^{13}C-^{13}C correlation spectrum of U-β_2m recorded with radio frequency-driven recoupling[34–36] (RFDR) employing a mixing period τ_{mix} = 1.76 ms. The resolution of this spectrum (natural line width ~ 0.5 ppm) is comparable to that observed in other amyloid fibril samples previously investigated by MAS NMR, including fibrils formed by TTR(105–115),[37] HET-s(218–289),[9] and PI3-SH3.[38] In this spectrum, primarily one-bond correlations are observed, potentially allowing the identification of different spin systems. For example, three Ile residues, one Ala, five Thr, and six Ser residues can be easily identified due to their characteristic chemical shifts.

Partial sequential assignments of the identified residues were obtained from NCACX and NCOCX correlations recorded with the U-β_2m fibril sample (Figure S2). These spectra display significant resonance overlap that limits the number of attainable unambiguous assignments. In order to improve the resolution of the spectra, we utilized the alternating and complementary labeling pattern exhibited by the 1,3-β_2m and 2-β_2m fibril samples. These samples contain very few directly bonded ^{13}C atoms, thus eliminating the CO-Cα and the Cα-Cβ J-couplings as a source of line broadening and decreasing the ^{13}C line widths to ~ 0.3 ppm. In addition, the absence of many one-bond ^{13}C-^{13}C couplings attenuates dipolar truncation effects.[39]

The reduced number of labeled spins in these samples further improves the resolution and simplifies the analysis of spectra like the ^{15}N-^{13}C correlations presented in Figure 2. These spectra were recorded using heteronuclear dipolar recoupling *via* TEDOR[40,41] with τ_{mix} = 1.6 ms, which is optimal for one-bond polarization transfer, i.e., N_i-CO_{i-1} and N_i-$C\alpha_i$. The improved line width allows the observation of certain cross-peaks that do not appear or are very weak in spectra recorded with uniformly labeled samples. For example, only two Gly residues are observed in U-β_2m spectra, while the NCA spectrum of 2-β_2m contains the three expected Gly cross-peaks. These one-bond ^{15}N-^{13}C correlations were complemented with medium range TEDOR experiments recorded with the 2-β_2m and 1,3-β_2m samples to acquire N_i-$C\alpha_{i-1}$, N_i-CO_i, and N_i-$C\beta_i$ correlations (Figure S3), while medium and long-range ^{13}C-^{13}C experiments (data not shown) were used to obtain $C\alpha_i$-$C\alpha_{i\pm1}$, CO_i-$C\beta_i$, CO_i-$C\gamma_i$, $C\alpha_i$-$C\gamma_i$, etc, correlations and to complete the sequential assignment of the resonances in LS β_2m fibrils. A detailed description of our resonance assignment strategy, with particular emphasis on samples prepared with [2-^{13}C] glycerol, will be given elsewhere.

All of the experiments used here for sequential assignments rely on the transfer of polarization mediated by the dipolar coupling between two spins, and therefore probe regions of the molecule that are characterized by high molecular order and low mobility. However, the number of well-resolved cross-peaks observed in the spectra, only accounts for a subset of the expected cross-peaks for a 100-residue protein. While static disorder can lead to line broadening and thus contribute to the broad background observed in some spectra (Figure 2), it is likely that the absence of cross-peaks or the differences in intensity and line width observed for some residues are due to dynamics. Motion in the kHz regime, for example, can interfere with cross polarization and ^{1}H decoupling and thus attenuate line intensities as well as produce broadening.[42–44] In the case of solution-like mobility, the dipole-dipole couplings required for efficient cross-polarization are attenuated and the

intensity of the resulting cross-peaks may be reduced. The absence of some regions of the sequence in MAS NMR spectra, originating from either of these three causes or a combination of them, has been observed in multiple amyloid fibril systems including Aβ,[45] α-synuclein,[13] Het-s(218–289),[46] and the Y145Stop variant of the human prion protein.[47,48]

Dynamics of the N-terminus of LS β_2m fibrils

To investigate the origins of the molecular disorder in the LS fibrils, we performed a MAS INEPT-TOBSY ^{13}C-^{13}C correlation experiment[49] and the spectra are presented in Figure 3. The INEPT step, commonly used in solution NMR experiments, is efficient only for highly mobile sites when applied to solid samples. These sites usually have vastly attenuated dipolar couplings that do not interfere with the J-coupling mediated polarization transfer during INEPT. The TOBSY (total through-bond correlation spectroscopy) mixing period relies only on the isotropic J-coupling to transfer polarization between the nearby ^{13}C spins. In the LS fibrils, six mobile spin systems can be identified, three of which include the backbone CO atoms. The chemical shifts of these spin systems are consistent with the random coil chemical shift values of Met, Ile, Gln, Arg, Thr and Lys, and, therefore, most likely arise from the first few N-terminal residues (MIQRTPK) of β_2m. The observed flexibility of the N-terminus is consistent with previous studies that indicate a high degree of solvent exposure for the first 20 residues.[26,50] Consistent with this, dipolar correlation ^{13}C-^{13}C spectra of a β_2m fibrillar sample that has been partially digested by pepsin, a process that is known to specifically cleave the N-terminal nine residues,[26,51] have the same number of cross-peaks as the ^{13}C-^{13}C spectra of undigested fibrils (data not shown). This observation confirms that the N-terminal residues have attenuated effective dipolar couplings and are not expected to appear in experiments based on dipolar mixing.

The dipolar and through-bond correlation experiments have allowed us to obtain spin system assignments for 64 of the 100 residues in LS β_2m fibrils. This includes 45 sequential assignments from dipolar spectra, 13 additional spin systems that are identified in dipolar spectra but not unambiguously assigned, and 6 mobile residues at the N-terminus. The sequentially assigned regions span residues 17–19, 27–32, 41–62, 71–74 and 77–86 that define the majority of the rigid fibril core. We estimate that the dipolar spectra contain additional cross-peaks consistent with the presence of approximately 10 more residues, which means that approximately 25 residues are not observed in any spectra. For example, while A78 gives well-resolved cross-peaks with sufficient intensity in all spectra, the other alanine residue, A15, is prominently missing. No residues have yet been identified in the region between I7 and E16, and in the C-terminus (L87–M99). No doubling of resonances has been observed, pointing towards the absence of polymorphism or heterogeneity in the case of these LS fibrils.

Chemical shift analysis of LS β_2m fibrils

The chemical shifts of 39 of the 45 sequentially assigned residues were analyzed with the TALOS program[52] and the Chemical Shift Index[53] (CSI) (Figure 4). TALOS provides predictions of the likely φ and ψ angles, while CSI gives an estimate of the secondary structure tendency based on the deviations of the chemical shifts from their random coil values. Six residues yielded no results due to incomplete assignments, and are excluded from Figure 4. Based on the predicted φ and ψ angles, and the chemical shifts of the Cα and Cβ atoms, three major β-strand regions can be identified amongst the assigned regions of the sequence, namely residues 28–32, 44–55 and 78–85. Comparison of the fibril β-strands with the native β-strands from both solution[54] and crystal structures,[55–57] shows that the native D-strand is extended in the fibrils, while strand F seems to be preserved (Figure 5). The residues around W60 and P72 probably also participate in β-strands, a major difference from the native structure.

Analysis of the Cβ and Cγ chemical shifts of the two assigned proline residues, P32 (ΔCβCγ = 4.3 ppm) and P72 (ΔCβCγ = 5.1 ppm), indicates that both residues are likely to adopt the more common *trans*-conformation in the fibril form.[58,59] This is in contrast to the native state of β_2m, where the H31-P32 bond is *cis*.[56,57] Although the exact conformation of the two proline residues can be determined only after the measurement of multiple distance constraints, the chemical shift data are consistent with biochemical experiments which indicate the presence of a *trans*-P32 folding intermediate on the fibril formation pathway at neutral pH,[60,61] while P32 is also likely to be predominantly in the *trans* form in the unfolded ensemble from which fibril formation is initiated at pH 2.5.

Comparison of the LS fibrils and the WL fibrils

The formation of fibrils with a different morphology dependent on the salt concentration, pH and temperature, is a characteristic feature of many amyloidogeneic proteins.[62] We investigated the structural and dynamic differences and similarities of the LS fibrils formed by β_2m at pH 2.5 and low ionic strength (50 mM), and the WL fibrils formed at pH 3.6 and high ionic strength (200 mM).[19] Buffers containing high concentrations of ions can significantly decrease the RF performance of conventional MAS NMR probes and increase the potential to overheat and damage the sample during data collection.[63] In order to avoid this problem, after formation and ultracentrifugation in 200 mM formate buffer, the WL fibrils were washed and repelleted in 50 mM buffer. The EM images of the fibrils before and approximately three weeks after the change of ionic strength did not reveal any detectable differences in their length and morphology (Figure S1).

Figure 6 compares 1D spectra recorded with CP (cross polarization) and INEPT ^{13}C magnetization preparation steps for both fibril forms. As was observed for the LS fibrils, the WL fibrils also contain a rigid fibril core as shown by their CP spectrum (Figure 6b), although the resolution of this spectrum is lower than that observed in the CP spectrum of the LS fibrils (Figure 6a). The INEPT spectrum of the WL fibrils (Figure 6d) contains more peaks than that of the LS fibrils (Figure 6c), indicating that the WL fibrils are characterized by enhanced mobility. Specifically, the WL fibrils seem to exhibit increased mobility in the backbone, as shown by the presence of more lines in the Cα region (40–60 ppm) of their INEPT spectrum, and in a few aromatic side-chains (110–140 ppm).

To compare the rigid cores of the two fibril forms, we recorded a ^{13}C-^{13}C correlation spectrum of the WL fibrils with τ_{mix} = 2.56 ms in an RFDR experiment. Figure 7 depicts a superposition of this spectrum with the RFDR spectrum of the LS fibrils (labels corresponding to the LS fibril assignments). The Cα-Cβ region of the WL fibrils is noticeably less resolved, and the relative intensities of some cross-peaks are significantly different. For example, only one of the five threonine residues present in the β_2m sequence (T73) appears as a clearly resolved peak in the WL fibril spectrum, while the unassigned serine Cα-Cβ cross-peak (marked with asterisks) is much stronger than in the LS fibril spectrum. On the other hand, the positions of many cross-peaks coincide for the two samples, including cross-peaks that belong to P32, S33, I46, K48, S52, A79, and V85 in the LS fibrils. These residues span all assigned regions of the LS fibrils, implying that the two fibril forms share a similar core. The WL fibrils, however, display a higher level of molecular disorder that compromises the resolution and the sensitivity of the dipolar spectra. This low sensitivity did not allow us to perform further experiments on this sample (Figure 6a and b). Nevertheless, our findings suggest that the rigid core of the WL fibrils may involve similar residues but is shorter in length than the core of the LS fibrils.

Discussion

The majority of residues are involved in the rigid core structure of LS β_2m fibrils

The MAS NMR assignments presented above describe the first such information obtained for LS amyloid-like fibrils formed from full-length oxidized β_2m. Although an MAS NMR study has been performed previously on amyloid-like fibrils formed from a short peptide fragment of β_2m (residues 20–41),[11] these fibrils do not form the disulphide bond between C25 and C80 known to be vital for amyloid formation of the intact protein, and lack the remainder of the sequence that is intimately involved in the fibril structure as shown by EPR, HX and proteolysis.[26,30,50] Furthermore, the 60–70 residue region has been shown by mutagenesis studies to be important in fibril formation from full-length β_2m under these conditions.[64,65] Although at low pH monomeric β_2m is found initially in an acid unfolded and highly dynamic state[21,22] approximately 70% of the residues* appear in dipolar spectra of the fibrils and most likely participate in the rigid fibril core. This implies that upon aggregation there is a substantial reorganization within the polypeptide chain, in agreement with previous studies using methods such as hydrogen exchange, limited proteolysis and EPR, which show that the majority of residues, particularly those located between C25 and C80, are involved in the fibril core.[25,26,30,66]

In our studies, a single set of resonances has been detected in MAS NMR spectra of LS fibrils, indicating that the observed residues reside in a homogeneous environment. Recently, a cryoEM study demonstrated that β_2m may form polymorphous LS fibril types under identical low pH conditions to those used here.[27] It was proposed that a complex architecture involving six protofilaments arranged as two crescent shaped units, each containing three protofilaments, formed and that within each protofilament there were at least three different subunit interfaces providing a complex superstructure. This is also demonstrated by the fact that hydrogen exchange studies of β_2m fibrils show that most backbone amide positions do not reach 100 % exchange, implying differing solvent exposure within a heterogeneous mixture where the same residue is protected differently depending on its molecular environment.[67,68] Such heterogeneity is also observed in EPR measurements of β_2m fibrils spin labeled at the N-terminal residues R3 and R11, where both mobile and immobile components contribute to the spectra, but not at any other regions of the protein involved in the core fibrillar structure.[30] In combination with previous studies, our MAS NMR data suggest that the core residues of β_2m are in a homogeneous protected environment in most fibrils and the gross physiognomic differences observed by cryoEM can be explained by the macroscopic arrangement of subunits and/or protofibrils in relation to each other. These interactions may create different chemical environments and conformational variations for amino acid segments involved in the subunit interfaces. Such conformational disorder can lead to line broadening and weak signal intensities as observed for a fraction of the residues in the protein (in addition to dynamics).

Analysis of the fibrils using TOBSY experiments that are particularly sensitive to dynamics within the sample indicated that six of the ~30 residues not observed in the dipolar experiments are highly mobile compared to the rest of the sequence. The amino acid types of the mobile residues correspond to those found within the seven N-terminal residues in the sequence. The fact that this segment of fibrillar β_2m is prone to specific cleavage at V9 by pepsin (a non-specific protease that has been shown to digest acid unfolded β_2m at over twenty sites throughout the sequence) suggests that this region of the polypeptide chain is solvent exposed and dynamic.[26,51,66] Indeed, Trp substitution and hydrogen exchange

*This estimate includes all observable residues in the dipolar spectra but not the 6 residues identified in through-bond (INEPT-TOBSY) experiments.

experiments of LS β_2m fibrils monitored by solution NMR spectroscopy have indicated that the N-terminus is exposed more than the rest of the protein, which is likely to be found in a protected core.[25,69] Interestingly, disruption of the N-terminal region of the native protein by mutation or truncation has also been observed to promote amyloid fibril formation at neutral pH.[60,61,70]

A recent study of the LS amyloid fibrils formed from β_2m at pH 2.5 using proteolysis and solution NMR spectroscopy has confirmed that residues 1–9 are cleaved by pepsin digestion and thus exposed, but are only seen to be dynamic by solution NMR when elongated with a sequence designed to favor random coil conformations.[51] It is likely that the discrepancy between the results presented here and the solution NMR dataset is due to the fact that the solution NMR study measured backbone amide dynamics while the MAS INEPT-TOBSY experiments described here were optimized for aliphatic transfer and were therefore more sensitive to side chain motion. Since the mobility detected here is only limited to the very end of the N-terminus, the rest of the 20 N-terminal residues that present increased HX exchange rates[50] could still be part of the fibril core or play a role in the intermolecular assembly of the fibrils. This possibility is also corroborated by EPR, a method that also probes side chain mobility, which indicates that spin labels at residues 3 and 11 are highly dynamic.[30]

β_2m is organized in a non-native manner in amyloid-like fibrils

The experiments discussed here, aided by the use of alternating labeling, have allowed the sequential assignment of 45 of the 100 residues present in the protein sequence and permit conclusions to be drawn concerning the structure of β_2m at an amino acid level within the fibril architecture. For instance, it is clear from the analysis of the chemical shifts (using TALOS and CSI) that the protein is organized in a non-native arrangement within these fibrils (Figures 4, 5). Comparison of the calculated secondary structure of β_2m in the LS fibrillar state with those from the native globular form (both free and MHC-bound) shows a number of differences, for instance regions of the protein sequence such as residues 59–60, 72–73 and 85–86 are found in β-sheet elements in the fibrillar state that are not present in the native state.[55–57] Throughout the central portion of the sequence of β_2m (residues ~28–86) where assignments are available there is an increased prevalence of amino acids showing a β-sheet conformational preference (except for residues 43 and 56). This agrees with previous data for β_2m as well as other amyloid-like states of proteins, provided by techniques such as X-ray diffraction, which show an increase in β-structure as the proteins form cross-β arrangements upon aggregation.[5] Furthermore, information from EPR and FTIR studies has also indicated that the β_2m polypeptide chain in LS fibrils is arranged in a parallel and in-register arrangement.[28,30] Interestingly, the region encompassing residues 44–55 is found in a β-sheet conformation in the LS fibrils yet this segment of the protein contains bulges and loops in most structural studies of native β_2m.[18] X-ray crystallography has indicated that rare conformations of the native state also exist where residues 51–56 of the protein form a continuous β-strand without the bulge,[56,70–72] although it has also been observed that straightening of β-strand D alone is insufficient for fibril formation.[73] These species have been proposed to be consistent with possible early structural changes that promote intermolecular strand-strand recognition in protein aggregation of β_2m at neutral pH.[70,74,75] However, it is worth noting that no crystal structure of β_2m shows the extensive β-strand conformational propensity that is indicated by the chemical shift data described here suggesting that increased β-sheet structure in this region of the sequence is promoted during the aggregation reaction.

An interesting feature of the MAS NMR data presented here is that both assigned prolines (P32 and P72) adopt the *trans* conformer in the fibrillar state. A number of studies have described the conformational change of the H31-P32 peptide bond from *cis* to *trans* as a

pivotal early step in the aggregation of β_2m at neutral pH.[20,61,70] At the low pH conditions under which fibrils were formed in this study it would be expected that this peptide bond would populate predominantly a *trans* configuration (in ~80 % of the acid unfolded molecules).[60,76] Therefore, the finding here that P32 adopts a *trans* conformation suggests that a *trans* P32 bond is a common feature of fibrils formed at both pH 2.5 and pH 7.

The divergence from native-like structure of the β_2m polypeptide chain in LS fibrils observed here is in good agreement with the cryoEM study of morphologically identical β_2m LS fibrils, which suggested that native-like monomers do not fit within the fibrillar architecture.[27] Other models founded on different types of biophysical information have also been proposed for LS fibrils formed from full-length β_2m. Based principally on analyses of the amyloid-forming abilities at low pH of variants of the human β_2m sequence, for instance, Ivanova and co-workers proposed that these fibrils are composed of a zipper-spine structure. In this model a tightly interdigitated core backbone is formed by residues 83–99 and the rest of the protein remains native-like and decorates the periphery of these fibrils.[77] Such an organization appears unlikely in the β_2m amyloid-like fibrils used in this study based on chemical shift analysis. Furthermore, a molecular dynamics study has proposed a domain swapping mechanism for propagation of β_2m fibrillation, where the N-terminal region of one monomer exchanges with that of another, leading to a chain reaction.[78] This model would lead to a native-like structure of β_2m, which is not easily reconciled with the MAS NMR data presented here. The presence of native-like monomers within LS β_2m fibrils would also contradict data obtained from fiber diffraction, FTIR and EPR experiments.[29,30,79]

A recently published MAS NMR study of full-length β_2m conjectured that the overall native structure is preserved in the fibrils, based on the observation of a fraction of similar ^{13}C signals between correlation spectra of fibrils formed at pH 2.5 and β_2m crystals.[80] In the absence of site-specific resonance assignments, such an inference is not consistent with the secondary structure in the fibril state presented in this article. The latter was derived from the analysis of chemical shifts in MAS spectra and shows important discrepancies between the fibrillar and native states. It may be possible that different fibril morphologies were studied in each case, as evidenced by large differences in MAS INEPT spectra, which in the sample analyzed here indicate a flexible N-terminus that is consistent with proteolysis and HX data.[25,26]

Different morphologies show different atomic level structure

The long-straight and twisted amyloid-like morphology of LS β_2m fibrils (~1 μm length) described above is thought to be structurally similar to *ex vivo* fibrillar samples extracted from DRA patients in that both structures give rise to the same characteristic FTIR spectrum and sensitivity to proteases.[29,81,82] In addition, the LS fibrils give rise to the full repertoire of structural, tinctorial and ligand binding properties of amyloid fibrils *ex vivo*, confirming their fidelity as good mimics of the naturally formed protein fibrils.[29] An atomic description of the LS fibrils may thus provide important insights into the structural properties of β_2m fibrils formed *in vivo*. In addition to this classical amyloid fibril type, β_2m can also form different fibril types when incubated at pH 2–4 *in vitro* at high ionic strength, resulting in WL fibrils. [83] The LS and WL fibrils are distinct classes and each is formed by divergent and competitive assembly pathways from the unfolded/partially folded monomers in equilibrium under the assembly conditions employed. As a consequence, the fibril type(s) that result from assembly can be modulated by alteration of the conditions under which the protein is incubated. Accordingly, pure LS fibrils form at low ionic strength and low pH, pure WL fibrils form at pH 3.6 at high ionic strength, while mixtures of the two are formed under conditions between these extremes.[83] Thus, by careful control of the solution conditions samples containing each morphologically dissimilar species can be prepared

exclusively (Figure S1). WL fibrils are a kinetically trapped species formed *via* a non-nucleated reaction, whereas the LS fibrils form with classic amyloid-like nucleation dependent kinetics.[19,64,83,84] The MAS NMR data presented here show that, in common with LS fibrils, WL fibrils exhibit a protected core that is rigid and hence amenable to solid-state NMR methods. Many chemical shifts located throughout the polypeptide sequence are similar to those found in LS fibrils, suggesting that there could be a high degree of structural similarity between these two fibril types. However, there are also differences between the spectra of LS and WL fibrils, which indicate that the WL fibrils are more dynamic and less organized than the LS fibrils. This agrees with hydrogen exchange and proteolysis data, which show that although WL fibrils have a protected core, it is not as extensive as that of LS fibrils.[25,26] Furthermore, experiments using densitometry indicate that WL fibrils have a strong core but a more loosely packed exterior than LS fibrils, consistent with the MAS NMR data presented here.[85] FTIR experiments also indicate that there are differences at an atomic level between LS and WL fibrils, in that different amide I′ absorbance maxima are observed.[29] In addition, recent studies using EPR, FTIR and Raman spectroscopies have proposed that the side chains of LS fibrils have a more fixed spatial arrangement in the core than those of WL fibrils.[30,86]

Importantly, the data presented here support the idea that the distinct macroscopic morphological features of the β_2m fibrils of different type, and perhaps the differences in their thermodynamic stability and reactivity to the amyloid specific dyes Congo Red and ThT as well as anti-amyloid antibodies,[24,83] result from variation in structure and dynamics at the molecular level, rather than from different association patterns starting from identical units. This is analogous to the fibril strain phenomena of prions, where the same protein sequences adopt alternative structures at a residue level leading to changes in fibril morphology, stability and ability to replicate.[87]

Conclusions

We have presented the initial MAS NMR spectra recorded from fibrils formed from full-length β_2m. The data indicate that LS fibrils formed under low pH conditions exhibit an extensive fibril core, however, there is a significant portion of the sequence (~25 of 100 residues) that is not observed in either dipolar or through-bond experiments. The N-terminal region is observed to display increased mobility compared with the remainder of the sequence, which may explain its susceptibility to proteolysis and HX. Residues 27–86 display increased β-sheet content in the fibrillar form consistent with a wealth of other biophysical data that indicate that the protein does not retain a native-like structure in these assemblies. Interestingly, the data reveal that the prolyl bond at residue 32 is found in a non-native *trans* conformation, consistent with proposed changes in early structures formed *en route* to aggregation at neutral pH.[20,70] The data indicate that the LS fibrils studied here contain a structurally unique and uniform organization within their core, and there is no evidence for gross structural polymorphism, at least within the regions of the sequence analyzed here. Finally, we show that the core structures of LS and WL β_2m fibrils appear to have common elements, although there remain substantial differences, most notably with regard to the increased dynamics and disorder displayed by the WL fibrils. Attainment of a model of the atomic structure of β_2m within amyloid-like fibrils will require completing the assignments using specifically labeled samples. Experiments to investigate the tertiary and quaternary structure of β_2m within the fibril architecture are currently underway in our laboratory.

Methods

Protein Expression and Purification

Recombinant human β_2-microglobulin (β_2m) was expressed in HCDM1 minimal media and purified as described elsewhere.[88] Uniformly ^{13}C- and ^{15}N-labelled β_2m samples were prepared by growing BL21(DE3) pLysS *Escherichia coli* in the presence of minimal media enriched with 1 gL^{-1} $^{15}NH_4Cl$ (Goss Scientific, UK) and 2 gL^{-1} D-glucose-$^{13}C_6$ (Sigma Aldrich, UK). Two biosynthetically site-directed ^{13}C-enriched samples were prepared by culturing bacteria in the presence of 1 gL^{-1} $^{15}NH_4Cl$ and either 2 gL^{-1} [1,3-^{13}C] glycerol or 2 gL^{-1} [2-^{13}C] glycerol and $NaH^{13}CO_3$ (Cambridge Isotope Laboratories, Andover, MA) to obtain labelling patterns consistent with those previously described.[31,32]

Fibril formation

Long, straight (LS) fibrils were formed at 1 mg ml^{-1} in 25 mM sodium acetate, 25 mM sodium phosphate, 0.04% (w/v) NaN_3 at pH 2.5, 37 °C with shaking for 14 days. The fibrils were centrifuged at 265,000 × *g* for 1 hr and the resulting hydrated pellet was transferred into a MAS rotor using a tabletop centrifuge. Varian 3.2 mm rotors (Revolution NMR, Fort Collins, CO) as well as Bruker 2.5 mm and 3.2 mm rotors (Bruker BioSpin, Billerica, MA) were used for the experiments outlined below. The rotors contained ~ 10 mg, 5 mg and 15 mg fibril sample respectively.

The worm-like (WL) fibrils were formed at 3 mg ml^{-1} in 200 mM ammonium formate buffer at pH 3.6, 37 °C with no shaking for 2 days. These fibrils were transferred in 50 mM ammonium formate buffer (pH 3.6) and centrifuged at 176,000 × *g* for 1 hr and packed into a Bruker 2.5 mm rotor.

Solid-state NMR spectroscopy

Experiments were performed with custom designed spectrometers (courtesy of D.J. Ruben, Francis Bitter Magnet Laboratory, Massachusetts Institute of Technology, Cambridge, MA) operating at 700 and 750 MHz ^1H Larmor frequency. The 700 MHz spectrometer was equipped with a triple-resonance $^1H/^{13}C/^{15}N$ Varian-Chemagnetics 3.2 mm probe (Varian, Inc., Palo Alto, CA). The 750 MHz experiments were performed with triple-resonance Bruker probes (Bruker BioSpin, Billerica, MA) equipped with a 2.5 mm coil or a 3.2 mm E-free coil. The sample was cooled with a stream of dry air maintained at a temperature of −5 °C, while we estimate that the sample temperature during the MAS experiments was 10–15 °C higher.

1D CP experiments were recorded using 1.2–1.8 ms contact time and 83 kHz TPPM[89] ^1H decoupling during acquisition. A 2D ^{13}C-^{13}C correlation experiment of the LS fibrils was recorded with an RFDR sequence with τ_{mix} = 1.76 ms at $\omega_r/2\pi$ = 18.2 kHz, with 40 kHz π pulses on the ^{13}C channel during mixing, and 83 kHz TPPM decoupling on the ^1H channel during evolution, mixing and acquisition. The acquisition time was 12.3 ms and 24 ms in the indirect and direct dimensions respectively. ^{15}N-^{13}C correlations on 2-β_2m and 1,3-β_2m LS fibril samples were recorded with TEDOR dipolar recoupling (τ_{mix} = 1.6 ms) at $\omega_r/2\pi$ = 10 kHz and 12.5 kHz respectively (40 kHz ^{15}N pulses, 100 kHz ^{13}C pulses and 83 kHz ^1H decoupling during mixing). The acquisition times were 12.8 ms for t_1 and 24 ms for t_2 for 2-β_2m, and 11.2 ms and 24 ms respectively for 1,3-β_2m fibrils. INEPT-TOBSY experiments were recorded at $\omega_r/2\pi$ = 16.667 kHz, TOBSY mixing without decoupling (τ_{mix} = 5.77 ms), 12 ms t_1 evolution and 24 ms t_2 evolution.

The ^{13}C-^{13}C correlation experiment of the WL fibrils was recorded with RFDR mixing (τ_{mix} = 2.56 ms) at $\omega_r/2\pi$ = 12.5 kHz, with 20 kHz π pulses on the ^{13}C channel during mixing, and

83 kHz ^{1}H decoupling during mixing and acquisition. The carrier frequency was centred on the aliphatic region. The acquisition time in the indirect dimension was 8 ms, and 24 ms in the direct dimension respectively.

Supplementary Material

Refer to Web version on PubMed Central for supplementary material.

Acknowledgments

We thank Dr. Patrick van der Wel, Dr. Kendra Frederick, and Matthew Eddy for insightful discussions and Ajay Thakkar and Michael Mullins for technical assistance. We acknowledge financial support from NIH grants EB003151 and EB002026, and the Wellcome Trust (grant numbers 075675 and 062164).

References

1. Westermark P, Benson MD, Buxbaum JN, Cohen AS, Frangione B, Ikeda SI, Masters CL, Merlini G, Saraiva MJ, Sipe JD. Amyloid. 2007; 14:179–183. [PubMed: 17701465]
2. Dobson CM. Nature. 2003; 426:884–890. [PubMed: 14685248]
3. Jimenez JL, Guijarro JL, Orlova E, Zurdo J, Dobson CM, Sunde M, Saibil HR. EMBO J. 1999; 18:815–821. [PubMed: 10022824]
4. Astbury WT, Beighton E, Parker KD. Biochim Biophys Acta. 1959; 35:17–25. [PubMed: 13794874]
5. Sunde M, Serpell LC, Bartlam M, Fraser PE, Pepys MB, Blake CCF. J Mol Biol. 1997; 273:729–739. [PubMed: 9356260]
6. LeVine H. Met Enzymol. 1999; 309:274–284.
7. Nelson R, Sawaya MR, Balbirnie M, Madsen AO, Riekel C, Grothe R, Eisenberg D. Nature. 2005; 435:773–778. [PubMed: 15944695]
8. van der Wel PCA, Lewandowski JR, Griffin RG. J Am Chem Soc. 2007
9. Wasmer C, Lange A, Van Melckebeke H, Siemer AB, Riek R, Meier BH. Science. 2008; 319:1523–1526. [PubMed: 18339938]
10. Petkova AT, Yau WM, Tycko R. Biochemistry. 2006; 45:498–512. [PubMed: 16401079]
11. Iwata K, Fujiwara T, Matsuki Y, Akutsu H, Takahashi S, Naiki H, Goto Y. Proc Natl Acad Sci USA. 2006; 103:18119–18124. [PubMed: 17108084]
12. Luca S, Yau WM, Leapman R, Tycko R. Biochemistry. 2007; 46:13505–13522. [PubMed: 17979302]
13. Heise H, Hoyer W, Becker S, Andronesi OC, Riedel D, Baldus M. Proc Natl Acad Sci USA. 2005; 102:15871–15876. [PubMed: 16247008]
14. Vilar M, Chou HT, Luhrs T, Maji SK, Riek-Loher D, Verel R, Manning G, Stahlberg H, Riek R. Proc Natl Acad Sci USA. 2008; 105:8637–8642. [PubMed: 18550842]
15. Cohen FE, Kelly JW. Nature. 2003; 426:905–909. [PubMed: 14685252]
16. Cherny I, Gazit E. Angew Chem, Int Ed. 2008; 47:4062–4069.
17. Gejyo F, Yamada T, Odani S, Nakagawa Y, Arakawa M, Kunitomo T, Kataoka H, Suzuki M, Hirasawa Y, Shirahama T, Cohen AS, Schmid K. Biochem Biophys Res Commun. 1985; 129:701–706. [PubMed: 3893430]
18. Saper MA, Bjorkman PJ, Wiley DC. J Mol Biol. 1991; 219:277–319. [PubMed: 2038058]
19. Radford SE, Gosal WS, Platt GW. Biochim Biophys Acta, Proteins Proteomics. 2005; 1753:51–63.
20. Eichner T, Radford SE. J Mol Biol. 2009; 386:1312–1326. [PubMed: 19452600]
21. Platt GW, McParland VJ, Kalverda AP, Homans SW, Radford SE. J Mol Biol. 2005; 346:279–294. [PubMed: 15663944]
22. Katou H, Kanno T, Hoshino M, Hagihara Y, Tanaka H, Kawai T, Hasegawa K, Naiki H, Goto Y. Protein Sci. 2002; 11:2218–2229. [PubMed: 12192077]

23. McParland VJ, Kad NM, Kalverda AP, Brown A, Kirwin-Jones P, Hunter MG, Sunde M, Radford SE. Biochemistry. 2000; 39:8735–8746. [PubMed: 10913285]
24. Smith DP, Jones S, Serpell LC, Sunde M, Radford SE. J Mol Biol. 2003; 330:943–954. [PubMed: 12860118]
25. Yamaguchi KI, Katou H, Hoshino M, Hasegawa K, Naiki H, Goto Y. J Mol Biol. 2004; 338:559–571. [PubMed: 15081813]
26. Myers SL, Thomson NH, Radford SE, Ashcroft AE. Rapid Commun Mass Spectrom. 2006; 20:1628–1636. [PubMed: 16636995]
27. White HE, Hodgkinson JL, Jahn TR, Cohen-Krausz S, Gosal WS, Muller S, Orlova EV, Radford SE, Saibil HR. J Mol Biol. 2009; 389:48–57. [PubMed: 19345691]
28. Fabian H, Gast K, Laue M, Misselwitz R, Uchanska-Ziegler B, Ziegler A, Naumann D. Biochemistry. 2008; 47:6895–6906. [PubMed: 18540682]
29. Jahn TR, Tennent GA, Radford SE. J Biol Chem. 2008; 283:17279–17286. [PubMed: 18424782]
30. Ladner CL, Chen M, Smith DP, Platt GW, Radford SE, Langen R. J Biol Chem. 2010; 285:17137–17147. [PubMed: 20335170]
31. LeMaster DM, Kushlan DM. J Am Chem Soc. 1996; 118:9255–9264.
32. Castellani F, van Rossum B, Diehl A, Schubert M, Rehbein K, Oschkinat H. Nature. 2002; 420:98–102. [PubMed: 12422222]
33. Castellani F, van Rossum BJ, Diehl A, Rehbein K, Oschkinat H. Biochemistry. 2003; 42:11476–11483. [PubMed: 14516199]
34. Bennett AE, Ok JH, Griffin RG, Vega S. J Chem Phys. 1992; 96:8624–8627.
35. Bennett AE, Rienstra CM, Griffiths JM, Zhen WG, Lansbury PT, Griffin RG. J Chem Phys. 1998; 108:9463–9479.
36. Bayro MJ, Ramachandran R, Caporini MA, Eddy MT, Griffin RG. J Chem Phys. 2008; 128:052321. [PubMed: 18266438]
37. Jaroniec CP, MacPhee CE, Bajaj VS, McMahon MT, Dobson CM, Griffin RG. Proc Natl Acad Sci USA. 2004; 101:711–716. [PubMed: 14715898]
38. Bayro MJ, Maly T, Birkett NR, Dobson CM, Griffin RG. Angew Chem, Int Ed. 2009; 48:5708–5710.
39. Bayro MJ, Huber M, Ramachandran R, Davenport TC, Meier BH, Ernst M, Griffin RG. J Chem Phys. 2009; 130:114506. [PubMed: 19317544]
40. Hing AW, Vega S, Schaefer J. J Magn Reson. 1992; 96:205–209.
41. Jaroniec CP, Filip C, Griffin RG. J Am Chem Soc. 2002; 124:10728–10742. [PubMed: 12207528]
42. Maus DC, Copie V, Sun BQ, Griffiths JM, Griffin RG, Luo SF, Schrock RR, Liu AH, Seidel SW, Davis WM, Grohmann A. J Am Chem Soc. 1996; 118:5665–5671.
43. Long JR, Sun BQ, Bowen A, Griffin RG. J Am Chem Soc. 1994; 116:11950–11956.
44. Bajaj VS, van der Wel PCA, Griffin RG. J Am Chem Soc. 2009; 131:118–128. [PubMed: 19067520]
45. Petkova AT, Ishii Y, Balbach JJ, Antzutkin ON, Leapman RD, Delaglio F, Tycko R. Proc Natl Acad Sci USA. 2002; 99:16742–16747. [PubMed: 12481027]
46. Siemer AB, Arnold AA, Ritter C, Westfeld T, Ernst M, Riek R, Meier BH. J Am Chem Soc. 2006; 128:13224–13228. [PubMed: 17017802]
47. Helmus JJ, Surewicz K, Nadaud PS, Surewicz WK, Jaroniec CP. Proc Natl Acad Sci USA. 2008; 105:6284–6289. [PubMed: 18436646]
48. Helmus JJ, Surewicz K, Surewicz WK, Jaroniec CP. J Am Chem Soc. 2010; 132:2393–2403. [PubMed: 20121096]
49. Andronesi OC, Becker S, Seidel K, Heise H, Young HS, Baldus M. J Am Chem Soc. 2005; 127:12965–12974. [PubMed: 16159291]
50. Hoshino M, Katou H, Hagihara Y, Hasegawa K, Naiki H, Goto Y. Nat Struct Biol. 2002; 9:332–336. [PubMed: 11967567]
51. Platt GW, Xue WF, Homans SW, Radford SE. Angew Chem, Int Ed. 2009; 48:5705–5707.
52. Cornilescu G, Delaglio F, Bax A. J Biomol NMR. 1999; 13:289–302. [PubMed: 10212987]

53. Wishart DS, Sykes BD. J Biomol NMR. 1994; 4:171–180. [PubMed: 8019132]
54. Verdone G, Corazza A, Viglino P, Pettirossi F, Giorgetti S, Mangione P, Andreola A, Stoppini M, Bellotti V, Esposito G. Protein Sci. 2002; 11:487–499. [PubMed: 11847272]
55. Khan AR, Baker BM, Ghosh P, Biddison WE, Wiley DC. J Immunol. 2000; 164:6398–6405. [PubMed: 10843695]
56. Trinh CH, Smith DP, Kalverda AP, Phillips SEV, Radford SE. Proc Natl Acad Sci USA. 2002; 99:9771–9776. [PubMed: 12119416]
57. Iwata K, Matsuura T, Sakurai K, Nakagawa A, Goto Y. J Biochem. 2007; 142:413–419. [PubMed: 17646174]
58. Sarkar SK, Torchia DA, Kopple KD, Vanderhart DL. J Am Chem Soc. 1984; 106:3328–3331.
59. Schubert M, Labudde D, Oschkinat H, Schmieder P. J Biomol NMR. 2002; 24:149–154. [PubMed: 12495031]
60. Kameda A, Hoshino M, Higurashi T, Takahashi S, Naiki H, Goto Y. J Mol Biol. 2005; 348:383–397. [PubMed: 15811375]
61. Jahn TR, Parker MJ, Homans SW, Radford SE. Nat Struct Mol Biol. 2006; 13:195–201. [PubMed: 16491092]
62. Andersen CB, Otzen D, Christiansen G, Rischel C. Biochemistry. 2007; 46:7314–7324. [PubMed: 17523599]
63. de Lacaillerie JBD, Jarry B, Pascui O, Reichert D. Solid State Nucl Magn Reson. 2005; 28:225–232. [PubMed: 16221542]
64. Platt GW, Routledge KE, Homans SW, Radford SE. J Mol Biol. 2008; 378:251–263. [PubMed: 18342332]
65. Routledge KE, Tartaglia GG, Platt GW, Vendruscolo M, Radford SE. J Mol Biol. 2009; 389:776–786. [PubMed: 19393661]
66. Monti M, Principe S, Giorgetti S, Mangione P, Merlini G, Clark A, Bellotti V, Amoresano A, Pucci P. Protein Sci. 2002; 11:2362–2369. [PubMed: 12237458]
67. Chatani E, Goto Y. Biochim Biophys Acta, Proteins Proteomics. 2005; 1753:64–75.
68. Yamaguchi K, Naiki H, Goto Y. J Mol Biol. 2006; 363:279–288. [PubMed: 16959264]
69. Kihara M, Chatani E, Iwata K, Yamamoto K, Matsuura T, Nakagawa A, Naiki H, Goto Y. J Biol Chem. 2006; 281:31061–31069. [PubMed: 16901902]
70. Eakin CM, Berman AJ, Miranker AD. Nat Struct Mol Biol. 2006; 13:202–208. [PubMed: 16491088]
71. Rosano C, Zuccotti S, Mangione P, Giorgetti S, Bellotti V, Pettirossi F, Corazza A, Viglino P, Esposito G, Bolognesi M. J Mol Biol. 2004; 335:1051–1064. [PubMed: 14698299]
72. Ricagno S, Colombo M, de Rosa M, Sangiovanni E, Giorgetti S, Raimondi S, Bellotti V, Bolognesi M. Biochem Biophys Res Commun. 2008; 377:146–150. [PubMed: 18835253]
73. Platt GW, Radford SE. FEBS Lett. 2009; 583:2623–2629. [PubMed: 19433089]
74. Richardson JS, Richardson DC. Proc Natl Acad Sci USA. 2002; 99:2754–2759. [PubMed: 11880627]
75. Benyamini H, Gunasekaran K, Wolfson H, Nussinov R. J Mol Biol. 2003; 330:159–174. [PubMed: 12818210]
76. Schmid FX. Methods Enzymol. 1986; 131:70–82. [PubMed: 3773774]
77. Ivanova MI, Sawaya MR, Gingery M, Attinger A, Eisenberg D. Proc Natl Acad Sci USA. 2004; 101:10584–10589. [PubMed: 15249659]
78. Chen YW, Dokholyan NV. J Mol Biol. 2005; 354:473–482. [PubMed: 16242719]
79. Jahn TR, Makin OS, Morris KL, Marshall KE, Tian P, Sikorski P, Serpell LC. J Mol Biol. 2010; 395:717–727. [PubMed: 19781557]
80. Barbet-Massin E, Ricagno S, Lewandowski JzR, Giorgetti S, Bellotti V, Bolognesi M, Emsley L, Pintacuda G. J Am Chem Soc. 132:5556–5557. [PubMed: 20356307]
81. Monti M, Amoresano A, Giorgetti S, Bellotti V, Pucci P. Biochim Biophys Acta. 2005; 1753:44–50. [PubMed: 16213198]

82. Relini A, De Stefano S, Torrassa S, Cavalleri O, Rolandi R, Gliozzi A, Giorgetti S, Raimondi S, Marchese L, Verga L, Rossi A, Stoppini M, Bellotti V. J Biol Chem. 2008; 283:4912–4920. [PubMed: 18056266]

83. Gosal WS, Morten IJ, Hewitt EW, Smith DA, Thomson NH, Radford SE. J Mol Biol. 2005; 351:850–864. [PubMed: 16024039]

84. Xue WF, Homans SW, Radford SE. Proc Natl Acad Sci USA. 2008; 105:8926–8931. [PubMed: 18579777]

85. Lee YH, Chatani E, Sasahara K, Naiki H, Goto Y. J Biol Chem. 2009; 284:2169–2175. [PubMed: 19017634]

86. Hiramatsu H, Lu M, Matsuo K, Gekko K, Goto YJ, Kitagawa T. Biochemistry. 2010; 49:742–751. [PubMed: 20028123]

87. Toyama BH, Kelly MJS, Gross JD, Weissman JS. Nature. 2007; 449:233–237. [PubMed: 17767153]

88. Kad NM, Thomson NH, Smith DP, Smith DA, Radford SE. J Mol Biol. 2001; 313:559–571. [PubMed: 11676539]

89. Bennett AE, Rienstra CM, Auger M, Lakshmi KV, Griffin RG. J Chem Phys. 1995; 103:6951–6958.

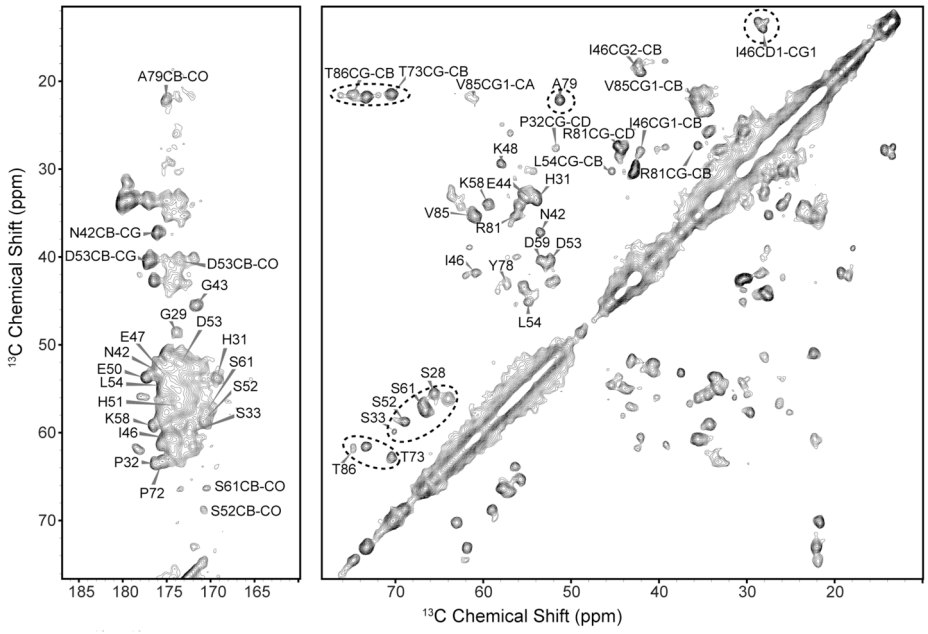

Figure 1.

^{13}C-^{13}C correlation spectrum (RFDR τ_{mix} = 1.76 ms) of LS U-β_2m fibrils, obtained at 750 MHz, $\omega_r/2\pi$ = 18.2 kHz. At this mixing time predominantly one-bond correlations are observed. Unless otherwise noted, the labels refer to Cα-CO correlations (left panel) and Cα-Cβ correlations (right panel). The circles show the regions where easy to identify residues like Ile, Ala, Thr, and Ser are typically found.

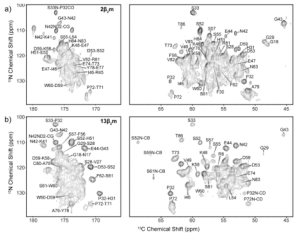

Figure 2.

^{15}N-^{13}C correlation spectra of a) 2-β_2m LS fibrils, obtained at 700 MHz, $\omega_r/2\pi$ = 10.0 kHz, and b) 1,3-β_2m LS fibrils, obtained at 750 MHz, $\omega_r/2\pi$ = 12.5 kHz. Dipolar recoupling was achieved with ZF-TEDOR and τ_{mix} = 1.6 ms. Unless otherwise noted, the labels refer to N_i-CO_{i-1} correlations (left panels) and N_i-$C\alpha_i$ correlations (right panels).

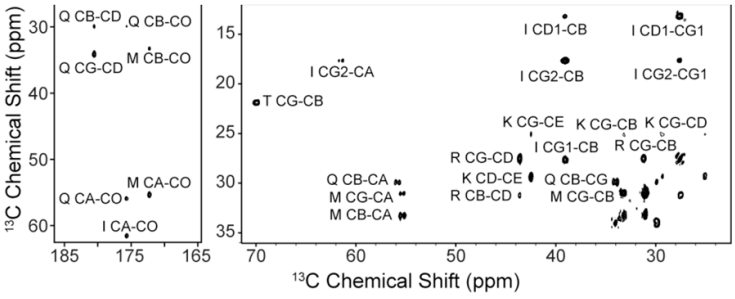

Figure 3.

^{13}C-^{13}C INEPT-TOBSY spectrum obtained at 750 MHz and $\omega_r/2\pi$ = 16.7 kHz with a U-β_2m LS fibril sample (τ_{mix} = 5.77 ms).

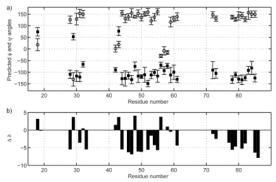

Figure 4.
Chemical shift analysis of the LS fibril assignments based on a) torsion angle analysis with TALOS and b) the chemical shift index (CSI). The circles in a) correspond to the predicted ψ angles, while the filled squares correspond to the predicted φ angles.

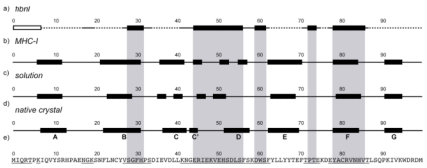

Figure 5.

a) Predicted β-strand regions (filled rectangles) in the fibrils, b) β-strands in β_2m bound to the heavy chain in the MHC-I complex [Ref. [56]], c) β-strands in native β_2m as determined by solution NMR [Ref. [55]], d) β-strands in native monomeric β_2m as determined by X-ray crystallography [Refs. [57] and [58]], e) the sequence of β_2m with all assigned residues in the fibril form underlined. The unfilled rectangle in a) represents the dynamic N-terminus. The designation of each native strand is shown in d).

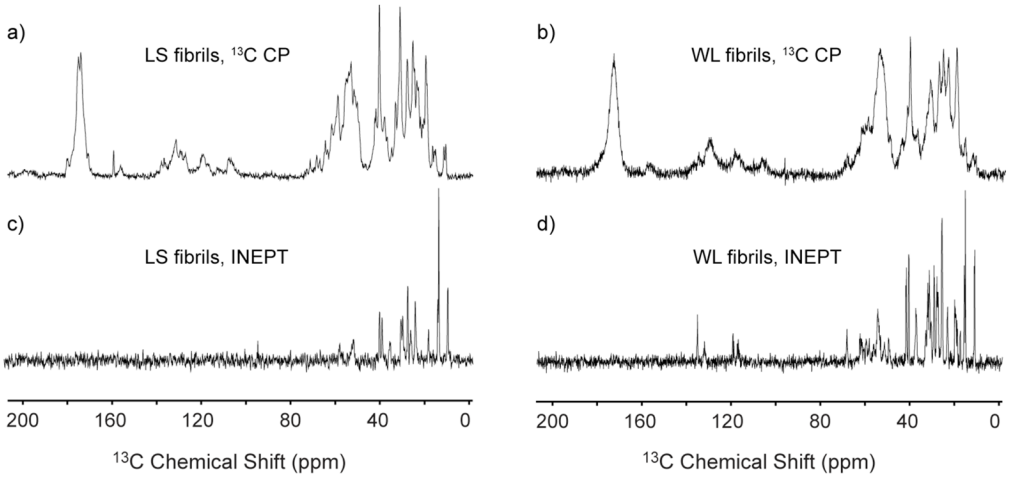

Figure 6.

Comparison of CP (a and b) and INEPT (c and d) spectra of the LS U-β_2m fibrils (a and c) and WL U-β_2m fibrils (b and d). All spectra were obtained at 750 MHz in a 2.5 mm rotor (~ 5 mg of sample). The spectra in a), b) and d) were recorded with $\omega_r/2\pi$ = 12.5 kHz and 128 scans, while c) was recorded with $\omega_r/2\pi$ = 16.7 kHz with 32 scans.

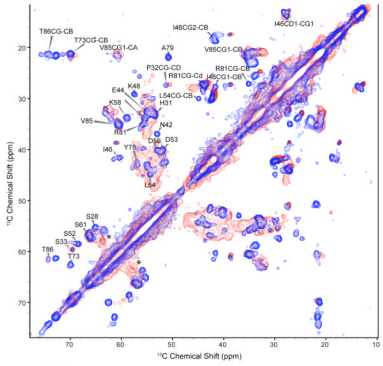

Figure 7.

^{13}C-^{13}C correlation spectra comparing U-β_2m WL (red) and U-β_2m LS fibrils (blue) (RFDR τ_{mix} = 2.56 ms, $\omega_r/2\pi$ = 12.5 kHz for the WL fibrils, and RFDR τ_{mix} = 1.76 ms, $\omega_r/2\pi$ = 18.182 kHz for the LS fibrils). The labels represent the LS fibril assignments. The asterisk denotes a Ser Cα-Cβ cross-peak that is much more prominent in the WL fibril spectrum.